Table 1. Tumor incidence and frequency in the gastrointestinal tract of Muc2 mice. Tumor incidence in wild-type and *Muc2*$^{-/-}$ mice was compared using the Mantel-Haenszel test, stratifying according to age at killing (6 month and 1 year). The risk of tumors was significantly greater in *Muc2*$^{-/-}$ than wild-type mice (odds ratio 8.956, $P < 0.0001$, Mantel-Haenszel test, StatXact, Cytel Software, Cambridge, MA). *n*, number of mice studied. Asterisk indicates mean ± SD.

Group (*n*)	No. mice with GI tumors			No. tumors per mouse		
	Total	Small intestine	Large intestine	Total	Small intestine	Large intestine
Muc2$^{+/+}$						
6 months (6)	0	0	0	0	0	0
1 year (18)	0	0	0	0	0	0
Muc2$^{-/-}$						
6 months (19)	3 (16%)	3 (16%)	0	0.32 ± 0.82*	0.32 ± 0.82	0
1 year (19)	13 (68%)	9 (47)	4 (21%)	1.58 ± 1.8	1.32 ± 1.8	0.26 ± 0.56

To assess the rate of migration of epithelial cells, we examined the fate of BrdU-labeled cells at 24 and 48 hours after BrdU injection. In the duodenum of wild-type mice, the majority of the cells had accumulated at the crypt-villous junction 24 hours after BrdU labeling (Fig. 1D). In contrast, in *Muc2*$^{-/-}$ mice, a large number of BrdU^{+} cells had migrated into the proximal portion of the villous. Within 48 hours, all the BrdU^{+} cells had been shed from the villi of *Muc2*$^{-/-}$ mice, whereas the majority of labeled cells were still present in the villi of wild-type mice (Fig. 1D). Similarly, at 24 hours the leading edge of BrdU^{+} cells was much higher up in the crypts of the distal colon of *Muc2*$^{-/-}$ mice, and within 48 hours positive cells were detected at the top of the crypts. In contrast, BrdU^{+} cells had migrated only three-quarters of the crypt length of the wild-type mice (Fig. 1E). Thus, epithelial cells migrated faster in the intestinal mucosa of *Muc2*$^{-/-}$ mice compared with wild-type mice.

Perturbation of the adenomatous polyposis coli (*APC*)–β-catenin pathway, as detected in familial adenomatous polyposis (FAP) patients and in the majority of sporadic colon cancers (*12*), results in nuclear accumulation of β-catenin and transcription of target genes including *c-myc* and *cyclin D1* (*13, 14*). Accordingly, tumors from *Apc1638* mice (*15*) showed strong nuclear expression of β-catenin and c-Myc (*6*), whereas tumors in *Muc2*$^{-/-}$ mice displayed a strong c-Myc signal that was not accompanied by alterations in the levels and distribution of β-catenin (*6*). The alteration of c-Myc expression was specific for tumor cells because the pattern of c-Myc in the normal intestinal mucosa of wild-type and mutant mice was not markedly different (*6*). These results were confirmed by Western blot analysis (*6*).

In summary, our data demonstrate that Muc2 functions in intestinal homeostasis and that its absence induces alterations that are manifested as increased proliferation, decreased apoptosis, and increased migration of intestinal epithelial cells. These alterations may be a secondary response to the absence of adequate protection and lubrication and/or a primary response to changes in Muc2 signaling. Inactivation of *Muc2* causes intestinal tumor formation with spontaneous progression to invasive carcinoma, and this occurs in the absence of the overt inflammatory response seen in other mouse models (*16–18*). The formation of rectal tumors also distinguishes the *Muc2*$^{-/-}$ mouse from previous rodent models of intestinal tumorigenesis, and this mouse may represent a useful model to study human rectal cancers, which are clinically distinct entities of cancer (*19*). The reduced representation of goblet cells is characteristic of many aberrant crypt foci (ACF) of both humans and rodents (*20, 21*), which are considered early preneoplastic lesions (*22–24*). Our data support the hypothesis that the reduction in these cells and, thus, reduction of the mucus they produce, plays a role in tumor formation. Lastly, this work suggests that analysis of *MUC2* expression may provide clinically useful information for prognosis and prevention of human colorectal cancer.

References and Notes

1. S. J. Gendler, A. P. Spicer, *Annu. Rev. Physiol.* **57**, 607 (1995).
2. Y. S. Kim, J. R. Gum, I. Brockhausen, *Glycoconj. J.* **13**, 693 (1996).
3. Y. S. Kim, J. R. Gum, *Gastroenterology* **109**, 999 (1995).
4. B. W. Van Klinken *et al.*, *Am. J. Physiol.* **276**, G115 (1999).
5. F. Aslam, L. Palumbo, L. H. Augenlicht, A. Velcich, *Cancer Res.* **61**, 570 (2001).
6. Supplementary figures and details of experimental procedures are available on *Science* Online at www.sciencemag.org/cgi/content/full/295/5560/1726/DC1.
7. B. Sands, D. Podolsky, *Annu. Rev. Physiol.* **58**, 253 (1996).
8. L. Shekels *et al.*, *Biochem. J.* **311**, 775 (1995).
9. L. L. Shekels *et al.*, *Biochem. J.* **330**, 1301 (1998).
10. S. Williams *et al.*, *J. Biol. Chem.* **276**, 18327 (2001).
11. A. Velcich *et al.*, data not shown.
12. L. Su *et al.*, *Science* **256**, 668 (1992).
13. T.-C. He *et al.*, *Science* **281**, 1509 (1998).
14. O. Tetsu, F. McCormick, *Nature* **398**, 422 (1999).
15. R. Fodde *et al.*, *Proc. Natl. Acad. Sci. U.S.A.* **91**, 8969 (1994).
16. U. Rudolph *et al.*, *Nature Genet.* **10**, 143 (1995).
17. M. Hermiston, J. Gordon, *Science* **270**, 1203 (1995).
18. S. Engle *et al.*, *Cancer Res.* **59**, 3379 (1999).
19. G. Steele *et al.*, *J. Am. Med. Assoc.* **264**, 1444 (1990).
20. K. Otori, K. Sugiyama, T. Hasebe, S. Fukushima, H. Esumi, *Cancer Res.* **55**, 4743 (1995).
21. T. Pretlow, W. Edelman, L. Hudson Jr., R. Kucherlapati, L. Augenlicht, *Proc. Am. Assoc. Canc. Res.* **38**, 126 (1997).
22. R. Bird, *Cancer Lett.* **37**, 147 (1987).
23. T. B. Pretlow *et al.*, *Cancer Res.* **51**, 1564 (1991).
24. I.-M. Siu *et al.*, *Cancer Res.* **59**, 63 (1999).

25. Supported by NIH grants CA 72835, CA 90808, and PO CA 13330. We thank S. Einherand, S. Gendler, G. Hansson, S. Ho, C. Tomasetto, and D. Podolsky for providing reagents; G. Cattoretti for suggestions on c-Myc immunohistochemistry; L. Klampfer for stimulating discussions; and J. Mariadason for critically reading the manuscript.

17 October 2001; accepted 25 January 2002

Postsynaptic Induction of BDNF-Mediated Long-Term Potentiation

Yury Kovalchuk, Eric Hanse,* Karl W. Kafitz, Arthur Konnerth†

Brain-derived neurotrophic factor (BDNF) and other neurotrophins are critically involved in long-term potentiation (LTP). Previous reports point to a presynaptic site of neurotrophin action. By imaging dentate granule cells in mouse hippocampal slices, we identified BDNF-evoked Ca^{2+} transients in dendrites and spines, but not at presynaptic sites. Pairing a weak burst of synaptic stimulation with a brief dendritic BDNF application caused an immediate and robust induction of LTP. LTP induction required activation of postsynaptic Ca^{2+} channels and *N*-methyl-D-aspartate receptors and was prevented by the blockage of postsynaptic Ca^{2+} transients. Thus, our results suggest that BDNF-mediated LTP is induced postsynaptically. Our finding that dendritic spines are the exclusive synaptic sites for rapid BDNF-evoked Ca^{2+} signaling supports this conclusion.

Neurotrophins promote neuronal survival and differentiation, but it has become increasingly clear that they also have essential roles in synaptic plasticity (*1–3*). Exogenous BDNF enhances transmission at the developing neuromuscular junction and at various central excitatory synapses (*4–8*). Furthermore, endogenous BDNF, via activation of the recep-

tor tyrosine kinase TrkB, can regulate induction of hippocampal LTP (*9–15*). Although the induction of LTP is generally believed to be postsynaptic (*16*, *17*), the facilitating action of BDNF on LTP induction is assumed to involve presynaptic mechanisms (*12*, *18*, *19*). This apparent contradiction resulted in the conclusion that "acute potentiation by neurotrophins cannot account for activity-induced LTP" in CA1 hippocampal pyramidal cells (*2*). Nevertheless, it has been suggested that BDNF regulates the induction of LTP by enhancing transmitter release during high-frequency synaptic stimulation (*12*, *20*, *21*). Furthermore, it is thought that the enhanced synaptic transmission produced by application of exogenous BDNF is expressed as a sustained enhancement of transmitter release (*5–7*, *19*). However, because the synaptic potentiation by BDNF has been provoked by a protracted (20 to 60 min) treatment of all elements in the neural tissue (*5*, *8*), the specific cellular mechanisms of BDNF in inducing synaptic plasticity remain elusive. It has been difficult to distinguish between the role of the suppression of inhibitory synaptic transmission (*22*, *23*) and the potential contribution of a general increase in neuronal excitability (*24*, *25*). Moreover, the potentiating effect of a prolonged exogenous BDNF exposure may depend on the exposure time (*6*), and it is sometimes difficult to reproduce (*3*).

To overcome some of these difficulties and limitations, we applied brief and targeted pulses of BDNF to mature dentate granule cells in mouse hippocampal slices. We mapped the effect of focal BDNF pulses on different compartments of dentate granule cells (Fig. 1A) (*26*). Application of BDNF to a granule cell body evoked a rapid depolarization, causing action potential firing (*27*), which was associated with a transient increase in Ca^{2+} concentration (Fig. 1B). The rapidly evoked BDNF response in granule cells was also induced by neurotrophin-4/5 and was blocked by the tyrosine kinase antagonist K252a (*26*).

BDNF pulses failed to induce any response when applied to the axon (Fig. 1B). The lack of BDNF-evoked responses in the axon was found in all four cells tested. By contrast, pulse-like BDNF applications (6 to 20 ms) to the dendrites evoked subthreshold depolarizations (7.7 ± 1.6 mV, n = 8 cells), which were associated with large Ca^{2+} signals (Fig. 1B). These signals were spatially restricted to a small portion of the dendrite (less than 30 μm) near the site of application (Fig. 1, C and D). The dendritic Ca^{2+} signals had amplitudes of 119 ± 22% [relative increase in fluorescence ($\Delta F/F$)], rise times of 82 ± 14 ms, and decay times of 536 ± 85 ms (n = 8 dendrites). When the cell was perfused with D890, a substance known to block voltage-gated calcium channels (*28*), the BDNF-evoked electrical response persisted (Fig. 1E), whereas the Ca^{2+} signal was abolished, even when long (20 ms) BDNF pulses producing an action potential were tested (n = 4 cells) (Fig. 1E). Furthermore, the BDNF-evoked Ca^{2+} transients were largely reduced (>70%) when the membrane potential (V_m) was clamped to −80 mV (n = 3 cells).

We next examined whether BDNF also activates dendritic spines. Spines were functionally identified by their Ca^{2+} responsiveness after synaptic stimulation of the afferent perforant path. A single excitatory postsynaptic potential (EPSP) evoked a prominent spine Ca^{2+} response ($\Delta F/F$ = 39 ± 2%, n = 4 spines) (Fig. 2, A and B). A paired synaptic stimulus caused a larger spine Ca^{2+} transient ($\Delta F/F$ = 91 ± 6%, n = 4 spines) with a signal component in the parent dendrite (Fig. 2B, lower traces). Similarly, a brief pulse (3 to 10 ms) of BDNF, applied locally to a spiny dendrite (Fig. 2C), produced Ca^{2+} signals in the dendrite and adjacent spines (Fig. 2D). These Ca^{2+} signals were associated with small somatic depolarizations (Fig. 2D, inset) of 3.2 ± 0.3 mV (n = 8 sites). An analysis of 19 spines at eight application sites (n = 6 cells) showed that BDNF consistently evoked larger Ca^{2+} signals in the spine than in the

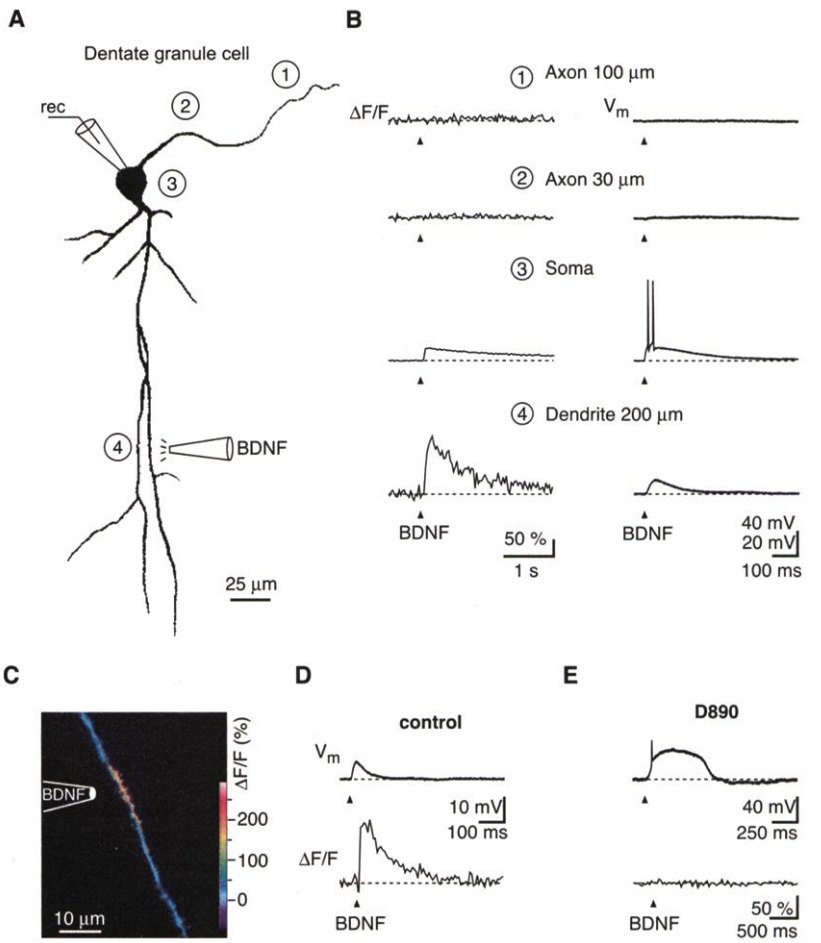

Fig. 1. Ca^{2+} signaling in dentate granule cells evoked by focal application of BDNF. (**A**) Reconstructed image of a granule cell with the whole-cell pipette and the BDNF-ejection pipette shown schematically. (**B**) BDNF-evoked fluorescence signals (left column, $\Delta F/F$) were recorded at four different locations in a granule cell, as indicated in (A) [in the axon (at sites 1 and 2), soma (at site 3), and distal dendrite (at site 4)]. Corresponding electrical recordings of V_m are shown on the right. Pulse durations were 10 ms (at site 4), 6 ms (at site 3), and 20 ms (at sites 1 and 2). Voltage scaling, 20 mV for sites 1, 2, and 4; 40 mV for site 3. (**C**) Pseudocolor image of a dendritic Ca^{2+} signal evoked by a BDNF pulse (10 ms). (**D**) BDNF-evoked Ca^{2+} transient (lower trace) from the active dendritic region shown in (C) and the associated electrical response (upper trace). (**E**) Block of the BDNF-evoked Ca^{2+} transient (lower trace) in another cell dialyzed with D890 (1 mM). Data in (A and B), (C and D), and (E) are from different cells. The V_m was −70 mV; the arrowheads indicate the time of application of BDNF (50 ng/ml). Each trace is an average of three consecutive trials.

Institut für Physiologie, Ludwig-Maximilians Universität München, 80336 München, Germany.

*Present address: Department of Physiology and Pharmacology, Göteborg University, 40530 Göteborg, Sweden.

†To whom correspondence should be addressed. E-mail: konnerth@lrz.uni-muenchen.de

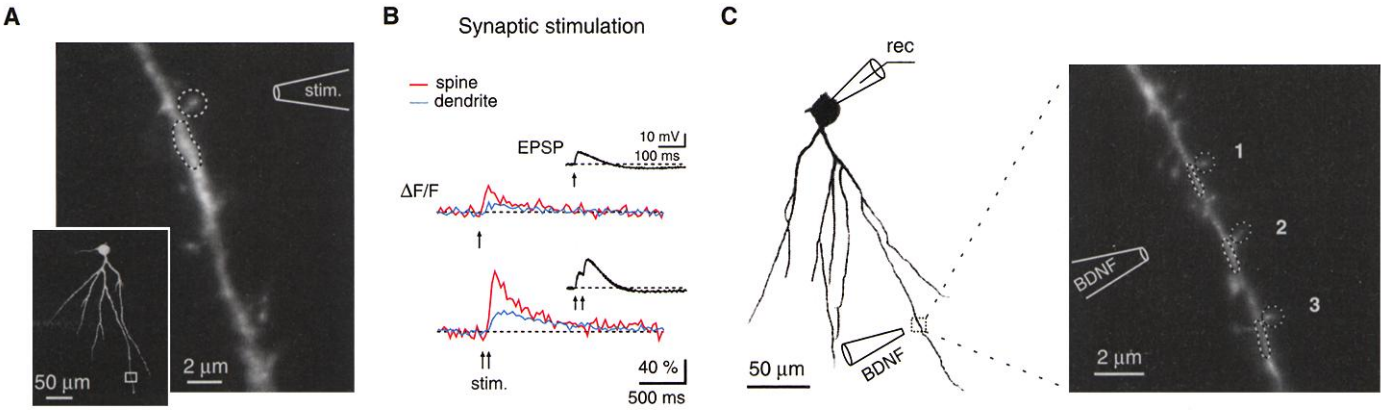

Fig. 2. BDNF-evoked and synaptically evoked Ca^{2+} signals in spines and dendrites. (**A**) Confocal image of a spiny dendrite and the schematically indicated positions of the pipette for synaptic stimulation. Inset, overview of the cell, reconstructed from confocal sections. The white box depicts the site of recording. (**B**) Ca^{2+} transients in the spine and in the adjacent dendrite from the regions marked in (A). The upper traces are the result of a single stimulus (arrow), and the lower ones resulted from a paired stimulation (20-ms interval) (pair of arrows). All traces are the averages of five consecutive trials. (**C**) Reconstructed image of a granule cell (left) and a spiny dendrite (right). The numbers correspond to three pairs of spino-dendritic regions of interest. The position of the BDNF-ejection pipette is as indicated. (**D**) BDNF-evoked (4-ms pulse) Ca^{2+} transients in three spines [red, regions from (C)] and in the adjacent dendritic regions [blue, regions from (C)]. The associated electrical signal is shown in the inset. (**E**) Plot of the spino-dendritic distribution of BDNF-evoked Ca^{2+} transients (n = 19 spino-dendritic pairs, six cells). The heavy line indicates the equal amplitude level in spine and dendrite. Inset, amplitudes in spines (red, n = 19 spines) normalized to the corresponding amplitudes obtained in the adjacent dendritic sites and the average dendritic reference amplitude (blue, n = 19 dendritic sites).

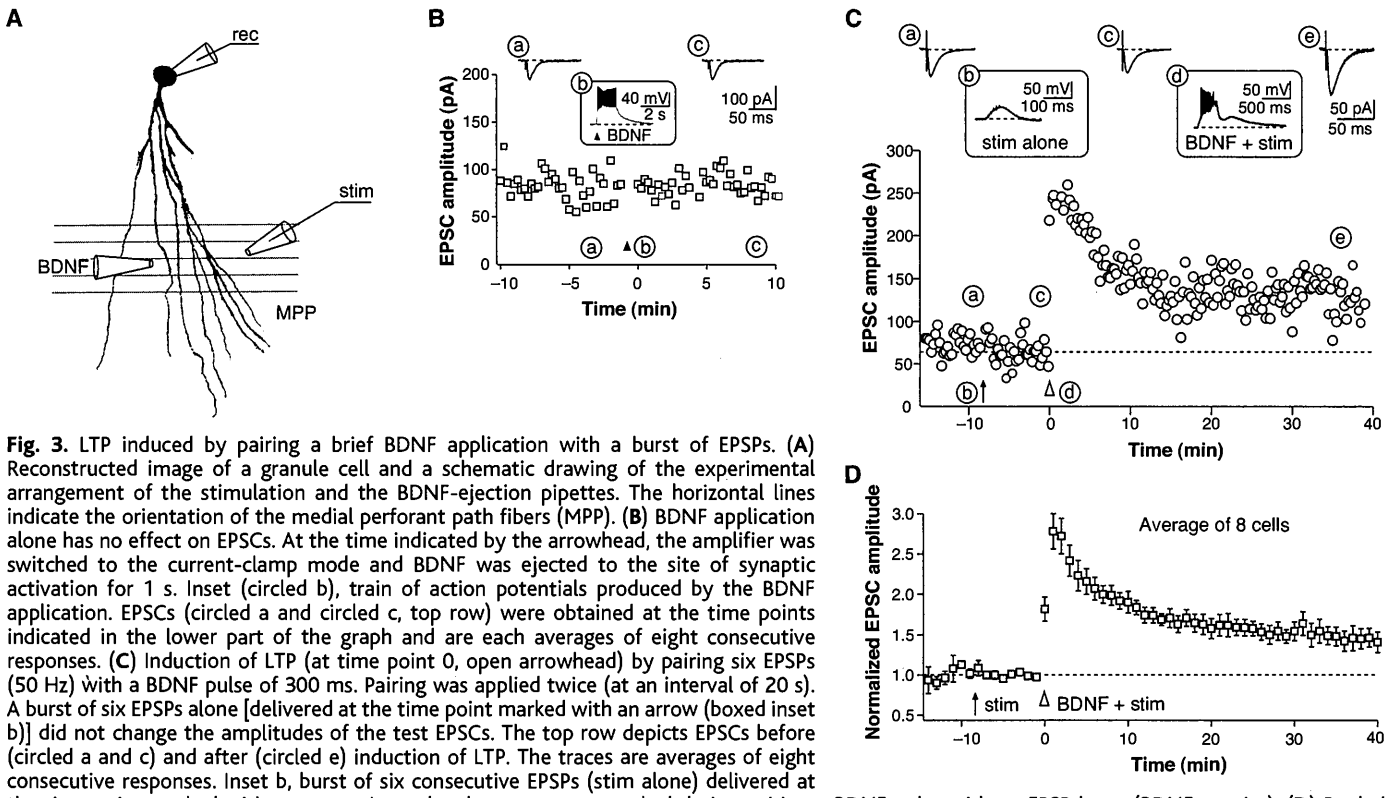

Fig. 3. LTP induced by pairing a brief BDNF application with a burst of EPSPs. (**A**) Reconstructed image of a granule cell and a schematic drawing of the experimental arrangement of the stimulation and the BDNF-ejection pipettes. The horizontal lines indicate the orientation of the medial perforant path fibers (MPP). (**B**) BDNF application alone has no effect on EPSCs. At the time indicated by the arrowhead, the amplifier was switched to the current-clamp mode and BDNF was ejected to the site of synaptic activation for 1 s. Inset (circled b), train of action potentials produced by the BDNF application. EPSCs (circled a and circled c, top row) were obtained at the time points indicated in the lower part of the graph and are each averages of eight consecutive responses. (**C**) Induction of LTP (at time point 0, open arrowhead) by pairing six EPSPs (50 Hz) with a BDNF pulse of 300 ms. Pairing was applied twice (at an interval of 20 s). A burst of six EPSPs alone [delivered at the time point marked with an arrow (boxed inset b)] did not change the amplitudes of the test EPSCs. The top row depicts EPSCs before (circled a and c) and after (circled e) induction of LTP. The traces are averages of eight consecutive responses. Inset b, burst of six consecutive EPSPs (stim alone) delivered at the time point marked with an arrow. Inset d, voltage response evoked during pairing a BDNF pulse with an EPSP burst (BDNF + stim). (**D**) Pooled data from eight experiments; the data points represent the average value of four consecutive responses.

adjacent dendrite. On average, the amplitude of the spine signal was 1.8 ± 0.2 times that of the dendritic signal (Fig. 2E, inset).

We next tested whether dendritic application of BDNF modifies glutamatergic synaptic transmission. Taking advantage of the rather strict laminar organization of the perforant path (*29*), we positioned the stimulation and BDNF-ejecting pipettes within the same beam of afferent fibers in the middle third of the molecular layer (Fig. 3A). This procedure allowed the ejected BDNF to reach the synapses that were activated by electrical stimulation. Application of BDNF alone did not modify the efficacy of synaptic transmission (Fig. 3B). However, a prominent synaptic potentiation was induced when the BDNF application was paired with an afferent burst of just five or six EPSPs (Fig. 3, C and D) (*30*). This weak synaptic stimulation was, by itself, insufficient to produce any potentiation (Fig. 3, C and D). The pairing-induced potentiation developed rapidly and peaked within 1 to 2 min to about 280% of the control (Fig. 3, C and D). The amplitude decayed toward a stable level of about 150% of the control within 30 to 40 min after the induction. We next established that BDNF mediates a strong facilitation of normal, tetanus-evoked LTP (*31*, *32*) rather than evoking a new form of LTP. Indeed, tetanus-evoked LTP completely occluded BDNF-mediated LTP (Fig. 4, A and B), and vice versa (Fig. 4, C and D). We also determined the time window during which the pairing must occur. There is no LTP induction if the electrical stimulation precedes the BDNF pulse by 200 ms (Fig. 4E). Instead, LTP is reliably induced during the standard "simultaneous" pairing protocol and, to a slightly decreased extent, if the burst stimulation follows the BDNF pulse within about 1 s (Fig. 4F). This poststimulation interval corresponds exactly to the period during which the postsynaptic cell is depolarized by BDNF. As soon as the V_m reaches its resting value (Fig. 4H, bottom panel), the pairing fails to induce LTP (Fig. 4G).

One mechanism by which BDNF might facilitate the induction of LTP is to enhance the synaptic response during high-frequency synaptic activation (*12*, *18*, *19*, *21*) by increased neurotransmitter release. We thus compared the synaptic burst response with and without simultaneous BDNF application (Fig. 5A). BDNF application did not enhance the burst-evoked synaptic response. On the contrary, both the amplitude of the first excitatory postsynaptic current (EPSC) and the overall charge mediated by the synaptic burst were reduced to a similar extent during the BDNF pulse (Fig. 5B). Thus, BDNF-mediated LTP induction is not likely to involve a presynaptic enhancement of the synaptic response during conditioning. We then tested the presynaptic BDNF responsiveness more directly in conditions in which both the afferent axons and the postsynaptic cells were loaded with a membrane-permeable Ca^{2+} indicator dye (*33*). (Fig. 5C). Although application of BDNF to the cell body of a granule cell produced a large BDNF-induced Ca^{2+} transient (Fig. 5D), BDNF had no effect on afferent axons and terminals (Fig. 5E). Both the postsynaptic (Fig. 5F) and presynaptic sites (Fig. 5G) displayed the expected action potential firing behavior. In addition, the presence of BDNF had no effect on burst stimulation–evoked presynaptic Ca^{2+} signals (Fig. 5E).

Our results suggest an exclusive postsynaptic site of Ca^{2+} signaling in response to

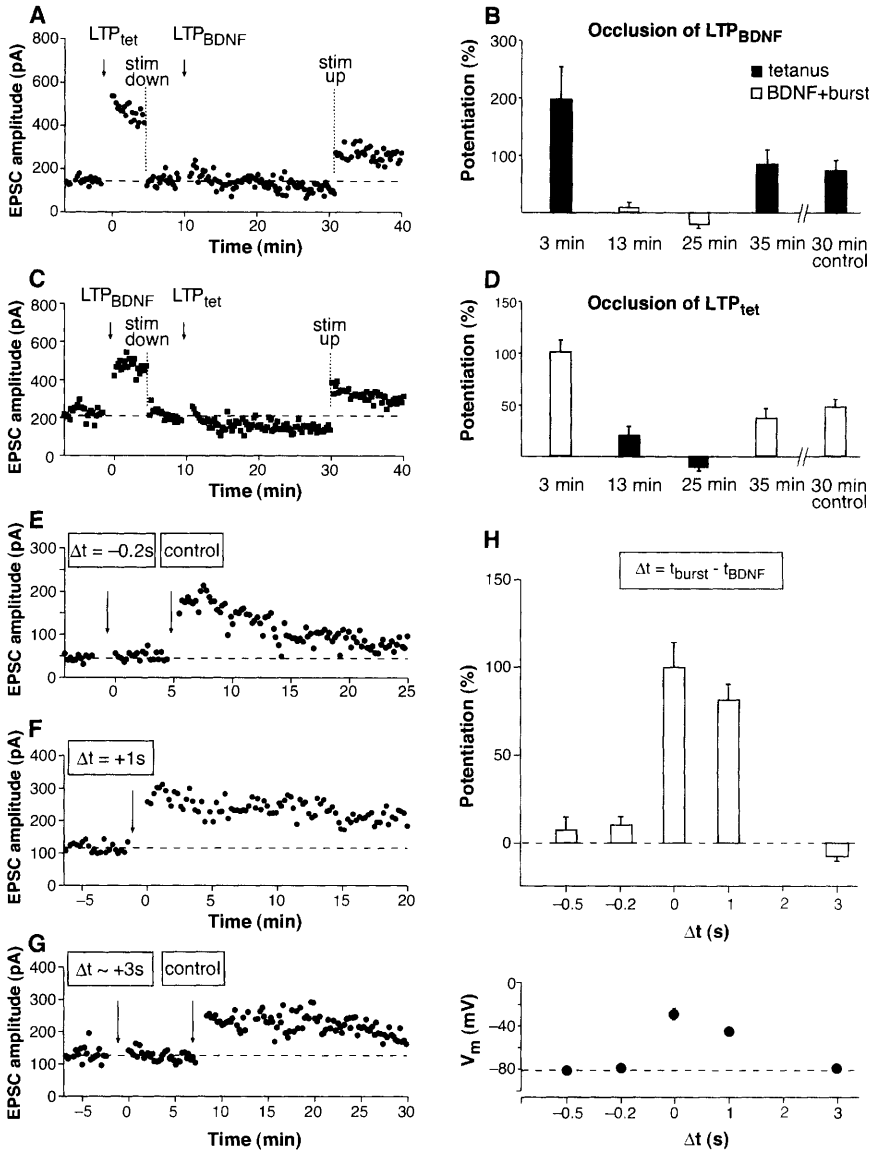

Fig. 4. (**A** to **D**) BDNF-induced LTP (LTP_{BDNF}) and tetanic stimulation–evoked LTP (LTP_{tet}) occlude each other. (A) LTP_{tet} occluded the induction of LTP_{BDNF}. Five min after the induction of LTP_{tet}, the stimulation intensity was reduced to obtain the EPSCs with amplitudes corresponding to the control values (stim down); at t = 30 min, the stimulation intensity was set to its initial value (stim up). Each data point reflects the amplitude of a single EPSC. (B) Mean change in EPSC amplitude (n = 4 experiments) measured at several relevant time points. The black bars correspond to the potentiation of EPSCs produced by tetanic stimulation just after the tetanus (3 min) and at t = 35 min. The white bars correspond to the relative change measured just after the attempt to induce LTP_{BDNF} (13 min) and at t = 25 min; "30 min control" indicates the potentiation by the LTP_{tet} protocol at 30 min in control experiments without any attempt to induce LTP_{BDNF} (n = 6 experiments). LTP_{tet} was induced by five bursts of 20 stimuli at 100 Hz delivered at intervals of 20 s, and the amplifier was switched to the current-clamp mode. (C and D) Similar experiments as in (A and B), but with a reversed order of LTP induction protocols. (**E** to **H**) The timing requirements for the induction of LTP_{BDNF}. (E to G) Electrical stimulation precedes the BDNF pulse by 0.2 s (E), follows it by 1 s (F), and follows that by about 3 s (G). The standard pairing protocol (control, Δt = 0) was applied to test the viability of the synaptic inputs (E and G). (H) The extent of potentiation (normalized to the control value, measured 3 min after LTP induction) for various time intervals Δt, as indicated. The lower graph shows the corresponding mean value of the V_m at the time just before the burst stimulation.

BDNF pulses and a direct role of this site in LTP induction. When the postsynaptic cell was dialyzed with the Ca^{2+} channel blocker D890, the conjunction of BDNF application and the brief afferent burst failed to induce any potentiation (Fig. 5, H and J). In the presence of the *N*-methyl-D-aspartate (NMDA) receptor antagonist 3-(2-carboxypiperazinyl) propyl-phosphate (CPP) (*34*), the conjunction resulted only in a transient potentiation and not in LTP (Fig. 5, I and J). Dialyzing the postsynaptic cell with the Ca^{2+} chelator 1,2-bis(2-aminophenoxy)ethane-*N*,*N*,*N*′,*N*′-tetraacetic acid (BAPTA) also prevented the induction of LTP (*35*). We verified the specificity of the BDNF action by showing that the BDNF scavenger molecule TrkB-IgG prevented the induction of BDNF-mediated LTP (*12*). A similar LTP-blocking action was also exerted by K252a, which suggests that LTP induction required phosphorylated TrkB receptors. Finally, we performed the present experiments in the presence of the γ-aminobutyric acid type A receptor antagonist bicuculline, excluding the possibility that the effects of BDNF were mediated through a modulation of synaptic inhibition (*22*, *23*).

BDNF-evoked dendritic excitation may serve as an instructive postsynaptic signal for

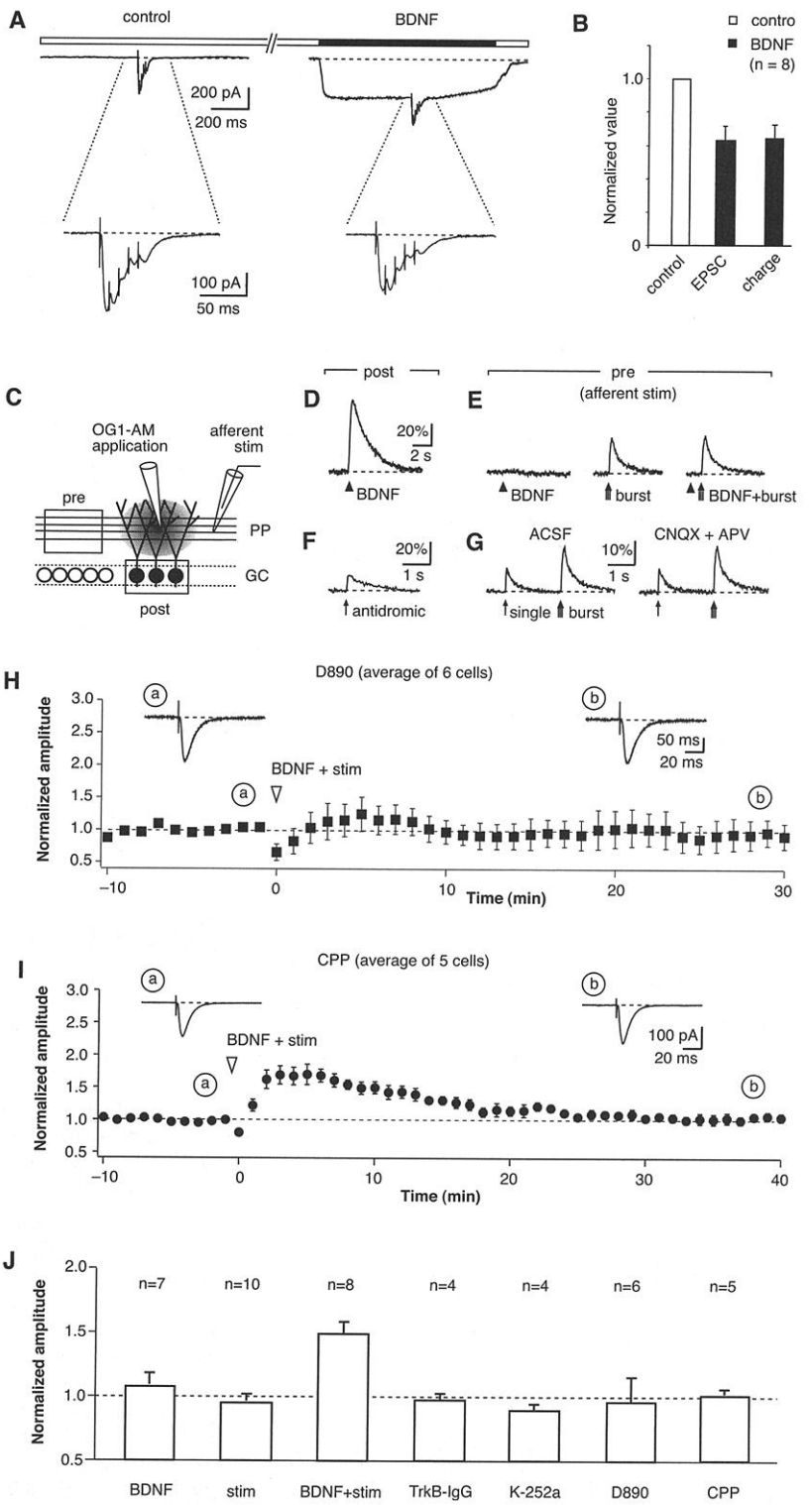

Fig. 5. Postsynaptic induction of BDNF-mediated LTP. (**A**) Comparison of an EPSC burst (five events at 50 Hz) obtained in the control and during the application of BDNF (50 ng/ml) for 1 s (solid bar). The pipette solution contained 2 mM D890. The traces are averages of four consecutive responses. (**B**) Summary results (n = 8 cells) of the BDNF-mediated reduction of the amplitude of the first EPSC of each burst (EPSC) and the charge of the total response (charge). (**C** to **G**) Post- and presynaptic Ca^{2+} signals in response to different stimuli. (C) Experimental arrangement. For indicator-dye delivery, the tip of an Oregon BAPTA1-AM–containing pipette was placed in the dendritic region of the dentate gyrus. The boxed region within the granule cell layer (GC) is the site of postsynaptic recording (post), and perforant path fiber (PP) activity was determined in the region marked "pre." (D and E) A BDNF pulse (20 ms) evoked a Ca^{2+} transient in the cell body of a granule cell (D) but failed to evoke a Ca^{2+} response presynaptically (E, left). A fiber-mediated Ca^{2+} transient (E, middle) produced by afferent stimulation (burst, five pulses at 100 Hz) was not affected by the presence of BDNF (50 ng/ml) (E, right). (F) Ca^{2+} transient produced by antidromic single-shock stimulation in granule cell bodies in which BDNF-mediated responses were also recorded (D). (G) Ca^{2+} transients recorded from axons and terminals in response to single-shock (single) and burst-afferent stimulation (burst). Ca^{2+} transients were not affected by the combination of 6-cyano-7-nitroquinoxaline-2,3-dione (10 μM) and D,L-2-amino-5-phosphonovaleric acid (50 μM). The data in (D to F) are from the same experiment. In (D to G), the traces are averages of three or four trials, and postsynaptic recordings are averages from three neighboring cell bodies. (**H**) Pooled data from six experiments showing block of the BDNF-mediated LTP by D890 (1 mM). (**I**) Pooled data from five experiments on the effect of CPP (10 μM) on BDNF-mediated LTP. In (H and I), the traces represent averages of eight consecutive EPSCs obtained from individual experiments. (**J**) Summary of the effect on synaptic transmission of BDNF application alone (BDNF), synaptic stimulation alone (stim), pairing of BDNF and synaptic stimulation (BDNF + stim), pairing after treating the slice with TrkB-IgG (5 ng/ml) for at least 1 hour (TrkB-IgG), pairing while the recording pipette contained D890 (D890), and pairing in the presence of 10 μM CPP (CPP). The amplitude values were obtained 30 min after the conditioning.

the induction of associative LTP. Such a role is also supported by recent experiments with a caged function–blocking antibody to BDNF (*36*), although the site of BDNF release is not clear yet. Although an autocrine action of postsynaptically released neurotrophin-4/5 has been proposed for the neuromuscular junction (*2*), there is evidence for an activity-dependent release of BDNF from presynaptic terminals in cortical neurons (*37*). A recent report (*38*) provides evidence for activity-dependent postsynaptic release of BDNF from cultured hippocampal neurons. However, because this BDNF release has not yet been directly correlated with LTP recordings, more work is required to determine whether, during LTP induction, BDNF is released from either pre- or postsynaptic compartments, or even from both compartments together.

Whatever the site of BDNF release, our results show that a brief BDNF pulse and a weak afferent burst robustly elicited LTP. Like tetanus-induced LTP (*16*, *17*), the induction of BDNF-mediated LTP required postsynaptic Ca^{2+} signaling (*39*) and NMDA receptor activation, as well as a close temporal association of pre- and postsynaptic activity. The mutual occlusion between BDNF-mediated and tetanus-evoked LTP suggests shared expression mechanisms. However, our results do not exclude a presynaptic expression of the BDNF-mediated LTP and are, therefore, not necessarily in contradiction with earlier evidence stressing the contribution of presynaptic mechanisms. An important conclusion of the present study is that spiny dendrites of mature dentate granule cells represent a highly responsive compartment for the rapid BDNF action. The block of this responsiveness prevented the induction of BDNF-mediated LTP. Our results reveal a critical mechanism underlying the surprisingly rapid, LTP-inducing action of BDNF and support an instructive role for BDNF in the induction of LTP in the mature brain.

References and Notes

1. H. Thoenen, *Science* **270**, 593 (1995).
2. A. F. Schinder, M.-m. Poo, *Trends Neurosci.* **23**, 639 (2000).
3. E. M. Schuman, *Curr. Opin. Neurobiol.* **9**, 105 (1999).
4. A. M. Lohof, N. Y. Ip, M.-m. Poo, *Nature* **363**, 350 (1993).
5. H. Kang, E. M. Schuman, *Science* **267**, 1658 (1995).
6. N. T. Sherwood, D. C. Lo, *J. Neurosci.* **19**, 7025 (1999).
7. A. F. Schinder, B. Berninger, M.-m. Poo, *Neuron* **25**, 151 (2000).
8. E. Messaoudi, K. Bardsen, B. Srebro, C. R. Bramham, *J. Neurophysiol.* **79**, 496 (1998).
9. M. Korte *et al.*, *Proc. Natl. Acad. Sci. U.S.A.* **92**, 8856 (1995).
10. S. L. Patterson *et al.*, *Neuron* **16**, 1137 (1996).
11. M. Korte *et al.*, *Proc. Natl. Acad. Sci. U.S.A.* **93**, 12547 (1996).
12. A. Figurov, L. D. Pozzo-Miller, P. Olafsson, T. Wang, B. Lu, *Nature* **381**, 706 (1996).
13. H. Kang, A. A. Welcher, D. Shelton, E. M. Schuman, *Neuron* **19**, 653 (1997).
14. G. Chen, R. Kolbeck, Y. A. Barde, T. Bonhoeffer, A. Kossel, *J. Neurosci.* **19**, 7983 (1999).
15. L. Minichiello *et al.*, *Neuron* **24**, 401 (1999).
16. B. Gustafsson, H. Wigström, *Trends Neurosci.* **11**, 156 (1988).
17. R. C. Malenka, J. A. Kauer, R. S. Zucker, R. A. Nicoll, *Science* **242**, 81 (1988).
18. B. Xu *et al.*, *J. Neurosci.* **20**, 6888 (2000).
19. J. N. Jovanovic, A. J. Czernik, A. A. Fienberg, P. Greengard, T. S. Sihra, *Nature Neurosci.* **3**, 323 (2000).
20. W. Gottschalk, L. D. Pozzo-Miller, A. Figurov, B. Lu, *J. Neurosci.* **18**, 6830 (1998).
21. L. D. Pozzo-Miller *et al.*, *J. Neurosci.* **19**, 4972 (1999).
22. M. Frerking, R. C. Malenka, R. A. Nicoll, *J. Neurophysiol.* **80**, 3383 (1998).
23. T. Tanaka, H. Saito, N. Matsuki, *J. Neurosci.* **17**, 2959 (1997).
24. E. S. Levine, C. F. Dreyfus, I. B. Black, M. R. Plummer, *Proc. Natl. Acad. Sci. U.S.A.* **92**, 8074 (1995).
25. H. E. Scharfman, *J. Neurophysiol.* **78**, 1082 (1997).
26. For electrophysiological methods used, see supplementary information on *Science* Online at www.sciencemag.org/cgi/content/full/295/5560/1729/DC1. All critical control experiments of the specificity of the rapid BDNF action performed previously for CA1 pyramidal cells (*27*) were repeated in dentate granule cells in hippocampal slices from adult mice and are also available on *Science* Online at the same address.
27. K. W. Kafitz, C. R. Rose, H. Thoenen, A. Konnerth, *Nature* **401**, 918 (1999).
28. Y. Kovalchuk, J. Eilers, J. Lisman, A. Konnerth, *J. Neurosci.* **20**, 1791 (2000).
29. P. Andersen, B. Holmquvist, P. E. Voorhoeve, *Acta Physiol. Scand.* **66**, 448 (1966).
30. For LTP experiments, afferent medial perforant path fibers were stimulated in the middle molecular layer at a frequency of 0.06 Hz, and synaptic responses were recorded in the voltage-clamp mode at a holding potential of −75 to −80 mV. After a stable baseline recording was obtained (for up to 20 min), LTP was induced by switching the amplifier to current-clamp mode and pairing the BDNF ejection pulse lasting for 300 to 600 ms with a burst stimulation (five or six stimuli at 50 Hz). The burst stimulation was delivered 50 ms before the end of the ejection pulse to ensure the coincidence of the synaptic responses with the moment of maximal concentration of BDNF at the synaptic site. Such pairing successfully evoked LTP even when executed once. Routinely, however, pairing was produced twice with an interval of 20 s to obtain a nearly saturating level of potentiation. It is noteworthy that such a BDNF-pairing protocol induced LTP also in hippocampal CA1 pyramidal cells [Web fig. 5 (*26*)]. Experiments in which the series resistance (R_s) was less than 20 megohms or in which R_s changed by more than 15% during the recording period were discarded. All data are expressed as mean ± SEM.
32. T. V. Bliss, T. Lømo, *J. Physiol. (London)* **232**, 331 (1973).
32. E. Hanse, B. Gustafsson, *J. Neurosci.* **12**, 3226 (1992).
33. Loading of perforant path axons and dentate granule cells with a Ca^{2+}-indicator dye was performed according to the protocol described in detail by Wu and Saggau (*41*) following a procedure pioneered by Regehr and Tank (*42*). Briefly, as indicated schematically in Fig. 5C, an Oregon BAPTA-1-AM (Molecular Probes, Inc., Eugene, OR) (0.9 mM in 10% dimethyl sulfoxide and 1% pluronic acid)–containing micropipette was positioned 100 to 200 μm below the slice surface into the molecular layer. After releasing dye by gentle-pressure application for about 30 s into the slice, the micropipette was withdrawn. This procedure yielded a robust and reproducible loading of axons far away from the site of dye ejection (>1 mm) and a dendritic loading of tens of granule cells.
34. B. U. Keller, A. Konnerth, Y. Yaari, *J. Physiol. (London)* **435**, 275 (1991).
35. Addition of 1 or 10 mM BAPTA to the pipette solution prevented LTP induction in six out of six granule cells.
36. A. H. Kossel, S. B. Cambridge, U. Wagner, T. Bonhoeffer, *Proc. Natl. Acad. Sci. U.S.A.* **98**, 14702 (2001).
37. K. Kohara, A. Kitamura, M. Morishima, T. Tsumoto, *Science* **291**, 2419 (2001).
38. M. Hartmann, R. Heumann, V. Lessmann, *EMBO J.* **20**, 5887 (2001).
39. H. Kang, E. M. Schuman, *Neurosci. Lett.* **282**, 141 (2000).
→ F. A. Edwards, A. Konnerth, B. Sakmann, T. Takahashi, *Pfluegers Arch. Eur. J. Physiol.* **414**, 600 (1989).
41. L. G. Wu, P. Saggau, *J. Neurosci.* **14**, 645 (1994).
42. W. G. Regehr, D. W. Tank, *J. Neurosci. Methods* **37**, 111 (1991).

43. We thank H. Thoenen, T. Bonhoeffer, O. Garaschuk, B. Gustafsson, and C. Rose for comments on early versions of the manuscript. Supported by grants from the Deutsche Forschungsgemeinschaft (A.K.).

6 November 2001; accepted 15 January 2002

Divided by Cytochrome Oxidase: A Map of the Projections from V1 to V2 in Macaques

Lawrence C. Sincich* and Jonathan C. Horton

Current models partition the primate visual system into dorsal (magno) and ventral (parvo, konio) streams. Perhaps the strongest evidence for this idea has come from the pattern of projections between the primary visual area (V1) and the second visual area (V2). Prior studies describe three distinct pathways: magno to thick stripes, parvo to pale stripes, and konio to thin stripes. We now demonstrate that V1 output arises from just two sources: patch columns and interpatch columns. Patch columns project to thin stripes and interpatch columns project to pale and thick stripes. Projection of interpatches to common V2 stripe types (pale and thick) merges parvo and magno inputs, making it likely that these functional channels are distributed strongly to both dorsal and ventral streams.

In primates, the pathway from the eye via the lateral geniculate nucleus to striate cortex is segregated along three lines: magnocellular, parvocellular, and koniocellular (*1*, *2*). The pathway from V1 to V2 is thought to perpetuate this division, by maintaining segregation of these three channels (*3*–*5*). Specifically, a magno-dominated pathway from layer 4B